

# Relativistic quasiparticle random-phase approximation description of isoscalar compression modes in open-shell nuclei in the $A \approx 60$ mass region

---

Paar, Nils; Vretenar, Dario; Nikšić, Tamara; Ring, Peter

Source / Izvornik: **Physical Review C - Nuclear Physics, 2006, 74**

Journal article, Published version

Rad u časopisu, Objavljena verzija rada (izdavačev PDF)

<https://doi.org/10.1103/PhysRevC.74.037303>

Permanent link / Trajna poveznica: <https://um.nsk.hr/um:nbn:hr:217:355220>

Rights / Prava: [In copyright](#) / [Zaštićeno autorskim pravom.](#)

Download date / Datum preuzimanja: **2024-09-25**



Repository / Repozitorij:

[Repository of the Faculty of Science - University of Zagreb](#)



# Relativistic quasiparticle random-phase approximation description of isoscalar compression modes in open-shell nuclei in the $A \approx 60$ mass region

N. Paar\*

*Institut für Kernphysik, Technische Universität Darmstadt, Schlossgartenstrasse 9, D-64289 Darmstadt, Germany and  
Physics Department, Faculty of Science, University of Zagreb, Zagreb, Croatia*

D. Vretenar and T. Nikšić

*Physics Department, Faculty of Science, University of Zagreb, Zagreb, Croatia*

P. Ring

*Physik-Department der Technischen Universität München, D-85748 Garching, Germany*

(Received 12 June 2006; published 26 September 2006)

Very recent inelastic  $\alpha$ -scattering data on the isoscalar monopole and dipole strength distributions in  $^{56}\text{Fe}$ ,  $^{58}\text{Ni}$ , and  $^{60}\text{Ni}$  are analyzed in the relativistic quasiparticle random-phase approximation (RQRPA) with the DD-ME2 effective nuclear interaction (nuclear matter compression modulus  $K_{\text{nm}} = 251$  MeV). The calculation nicely reproduces the observed asymmetric shapes of the monopole strength, and the bimodal structure of the dipole strength distributions. The RQRPA centroid and mean energies are in very good qualitative agreement with the experimental values both for the monopole, and for the low- and high-energy components of the dipole transition strengths. It is noted, however, that while DD-ME2 reproduces in detail the excitation energies of the giant monopole resonances (GMR) in nuclei with  $A \geq 90$ , the theoretical centroids are systematically above the experimental values in lighter nuclei with  $A \leq 60$ . The latter can be reproduced with an effective interaction with a lower value of  $K_{\text{nm}} \approx 230$  MeV but, because of the asymmetric shapes and pronounced fragmentation of the monopole strength distributions, isoscalar GMR data in light nuclei cannot provide accurate estimates of the nuclear matter compression modulus.

DOI: [10.1103/PhysRevC.74.037303](https://doi.org/10.1103/PhysRevC.74.037303)

PACS number(s): 21.60.Ev, 21.60.Jz, 21.65.+f, 24.30.Cz

Compressional modes in atomic nuclei can be used to deduce the value of the nuclear matter compression modulus  $K_{\text{nm}}$  from a comparison of experimental excitation energies with those predicted by microscopic nuclear effective interactions [1]. Inelastic  $\alpha$ -scattering experiments have been employed in high precision studies of the systematics of isoscalar giant monopole resonance (ISGMR) in nuclei with  $A \geq 90$ . There is much less experimental information, and only few microscopic theoretical analyses of the structure of compressional modes in lighter nuclei with  $A < 90$ . While in heavy nuclei the shape of the ISGMR strength distribution is typically symmetric, for  $A < 90$  the ISGMR display asymmetric shapes with a slower slope on the high energy side of the peak, and with a further decrease of the mass number the ISGMR strength distributions become strongly fragmented. An interesting question, of course, is whether studies of compressional vibrations in lighter nuclei can provide additional information on the nuclear matter compression modulus. Namely,  $K_{\text{nm}}$  corresponds to bulk nuclear compressibility, whereas one expects that surface compressibility plays an increasingly important role in the structure of ISGMR in lighter systems. Recently the isoscalar giant resonances in  $^{56}\text{Fe}$ ,  $^{58}\text{Ni}$ , and  $^{60}\text{Ni}$  have been studied with small-angle inelastic  $\alpha$ -scattering [2]. Since there were no specific microscopic calculations of E0 and E1 strength distributions in  $^{56}\text{Fe}$  and  $^{60}\text{Ni}$ , the mass

dependence of the ISGMR excitation energies between  $A = 40$  and  $A = 90$  was thus compared with results of leptodermous expansions based on Hartree-Fock + RPA calculations with Skyrme interactions [3], and constrained relativistic mean-field calculations [4]. The purpose of this work is to perform fully self-consistent relativistic quasiparticle random-phase approximation (RQRPA) calculations of isoscalar E0 and E1 strength distributions in  $^{56}\text{Fe}$ ,  $^{58}\text{Ni}$ , and  $^{60}\text{Ni}$ , using a modern effective density-dependent interaction which is known to reproduce the systematics of compressional modes in heavier nuclei with  $A \geq 90$ . However, one should note that RPA, being a small amplitude limit of the time dependent mean field theory, is somewhat less reliable for lighter systems and the coupling to more complex configurations might also be more important.

Recent theoretical studies of nuclear compressional modes include the fluid dynamics approach [5], the Hartree-Fock + RPA with Skyrme interactions [6–9], the RPA based on separable Hamiltonians [10], linear response within a stochastic one-body transport theory [11], the relativistic transport approach [12], and the self-consistent relativistic RPA [13–16]. As has been pointed out by Shlomo *et al.*, however, most current implementations of the nonrelativistic RPA are not self-consistent, and based on numerous approximations [7]. In several following publications the consequences of violation of self-consistency on the properties of giant resonances have been investigated in a systematic manner [17–19]. Very recent studies have emphasized the importance of a fully self-consistent description of ISGMR, and confirmed that

\*Electronic address: [nils.paar@physik.tu-darmstadt.de](mailto:nils.paar@physik.tu-darmstadt.de)

the low value of  $K_{\text{nm}} = 210\text{--}220$  MeV, previously obtained with Skyrme functionals, is an artefact of the inconsistent implementation of effective interactions [9,20]. The excitation energies of the ISGMR in heavy nuclei are thus best described with Skyrme and Gogny effective interactions with  $K_{\text{nm}} \approx 235$  MeV. In Refs. [8,9] it has been shown that it is also possible to construct Skyrme forces that fit nuclear ground state properties and reproduce ISGMR energies, but with higher values of  $K_{\text{nm}}$ . However,  $K_{\text{nm}} > 240$  MeV would require unrealistically large value of the symmetry energy at saturation density  $a_4$  [9]. A recent relativistic RPA analysis has shown that only effective interactions with  $K_{\text{nm}} = 250\text{--}270$  MeV reproduce the experimental excitation energies of ISGMR in medium-heavy and heavy nuclei [16].

Data on the compressional isoscalar giant dipole resonance (ISGDR) could also be used to constrain the range of allowed values of  $K_{\text{nm}}$  [21,22]. The problem, however, is that the isoscalar E1 strength distributions display a characteristic bimodal structure with two broad components. Theoretical analyses have shown that only the high-energy component represents compressional vibrations [23,24], whereas the broad structure in the low-energy region corresponds to vortical nuclear flow associated with the toroidal dipole moment [25–27]. A strong mixing between compressional and vorticity vibrations in the isoscalar E1 states can be expected up to the highest excitation energies in the region  $\approx 3\hbar\omega$  [26,27]. Nevertheless, models which use effective interactions with  $K_{\text{nm}}$  adjusted to ISGMR excitation energies in heavy nuclei, also reproduce the structure of the high-energy portion of ISGDR data [7,28,29].

In this work the isoscalar E0 and E1 strength distributions for the open-shell nuclei  $^{56}\text{Fe}$ ,  $^{58}\text{Ni}$ , and  $^{60}\text{Ni}$  are calculated in the RQRPA [30] formulated in the canonical single-nucleon basis of the relativistic Hartree-Bogoliubov (RHB) model [31]. This approach is fully self-consistent: the same interactions, in the particle-hole and particle-particle channels, are used both in the RHB equations that determine the canonical quasiparticle basis, and in the RQRPA equations. In this way, we ensure that RQRPA amplitudes do not contain spurious components associated with the mixing of the nucleon number in the RHB ground state, or with the center-of-mass translational motion.

In Fig. 1 we display the isoscalar monopole strength distributions for  $^{56}\text{Fe}$ ,  $^{58}\text{Ni}$ , and  $^{60}\text{Ni}$ . The RHB+RQRPA calculation has been performed with the DD-ME2 effective interaction in the particle-hole channel and the finite-range Gogny force has been used in the particle-particle channel [32]. DD-ME2 belongs to a new class of relativistic effective nuclear interactions with density-dependent meson-nucleon vertex functions, providing a realistic description of asymmetric nuclear matter, neutron matter and finite spherical and deformed nuclei. For DD-ME2 the nuclear matter compression modulus amounts  $K_{\text{nm}} = 251$  MeV. The strength distributions in Fig. 1 can be compared with the data from Ref. [2] (Figs. 8, 9, and 10). In all three nuclei the calculation predicts asymmetric shapes for the isoscalar E0 strength distributions, in agreement with data. In particular, an additional tail in the transition strength is obtained above the main ISGMR peaks for  $^{56}\text{Fe}$  and  $^{60}\text{Ni}$ . For  $^{58}\text{Ni}$  most of the strength is distributed over two

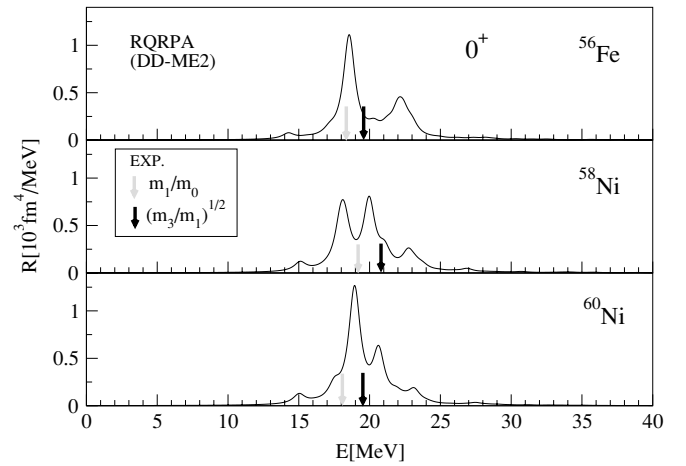


FIG. 1. The RQRPA(DD-ME2) isoscalar monopole strength distributions in  $^{56}\text{Fe}$  and  $^{58,60}\text{Ni}$  in comparison with the experimental centroid  $m_1/m_0$  and mean  $\sqrt{m_3/m_1}$  energies [2].

major peaks, with an additional pronounced high-energy tail. The arrows denote the positions of the experimental centroid ( $\bar{E}_1 = m_1/m_0$ ) and mean energies ( $\bar{E}_3 = \sqrt{m_3/m_1}$ ), where  $m_k = \int E^k R(E) dE$  are the energy moments, and  $R(E)$  is the transition strength distribution function. We note that in all three nuclei the main ISGMR peak predicted by the RQRPA calculation is located in the narrow energy window between the  $\bar{E}_1$  and  $\bar{E}_3$  experimental energies.

In the upper panel of Fig. 2 we plot the RHB+RQRPA results for the ISGMR centroid energies of a series of spherical nuclei from  $^{40}\text{Ca}$  to  $^{208}\text{Pb}$ , calculated with the DD-ME2 effective interaction, in comparison with data from the Texas A&M University (TAMU) [2,33–35] and Osaka [28,29] compilations. We note that the latter data correspond to

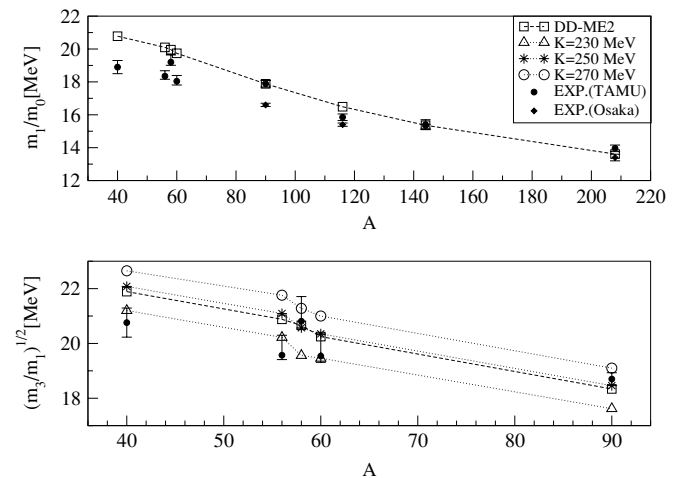


FIG. 2. (Upper panel) The RQRPA centroid energies of ISGMR in  $40 \leq A \leq 208$  nuclei in comparison with TAMU [2,33–35] and Osaka [28,29] data compilations. (Lower panel) The calculated mean energies of ISGMR for several medium-mass nuclei in comparison with the data from Ref. [2]. In addition to DD-ME2, three additional effective interactions with the values of  $K_{\text{nm}} = 230, 250,$  and  $270$  MeV [16] have been used.

peak energies and, especially in nuclei in which a high-energy tail is found above the main peak, these values should be somewhat below the TAMU centroid energies. The agreement between the excitation energies calculated with DD-ME2 and the TAMU data is remarkable for nuclei with  $A \geq 90$ , whereas the theoretical centroids are systematically above the experimental values in lighter nuclei. The origin of this discrepancy is not understood, but it could be due to the fact that in light nuclei the surface incompressibility plays a more important role in determining the ISGMR, whereas  $K_{\text{nm}}$  represents the volume incompressibility. The former quantity is seldom taken into account when adjusting the parameters of an effective interaction and, therefore, we do not really expect that DD-ME2 can reproduce in detail the moments of asymmetric and even fragmented isoscalar E0 strength distributions in light nuclei with  $A \leq 60$ .

It seems that data on ISGMR in light nuclei are not very useful in extracting information on the nuclear matter compression modulus  $K_{\text{nm}}$ . Nevertheless, we have tried to reproduce these data with few additional effective interactions. In the recent analysis of nuclear matter incompressibility in the relativistic mean-field framework [16], families of density-dependent interactions with different values of the nuclear matter compression modulus  $K_{\text{nm}}$  and symmetry energy at saturation (volume asymmetry)  $a_4$ , were adjusted to reproduce nuclear matter and ground-state properties of spherical nuclei. By performing fully consistent R(Q)RPA calculations of isoscalar E0 and isovector E1 strength distributions in spherical nuclei with  $A \geq 90$ , it has been shown that the comparison with data restricts the values of  $K_{\text{nm}}$  to  $\approx 250\text{--}270$  MeV, and the range of volume asymmetry to  $32 \text{ MeV} \leq a_4 \leq 36 \text{ MeV}$ . A weak correlation between  $a_4$  and  $K_{\text{nm}}$  was found, i.e., interactions with lower volume asymmetry allow for slightly lower values of  $K_{\text{nm}}$ . Therefore in addition to DD-ME2, the family of interactions with  $a_4 = 32$  MeV and  $K_{\text{nm}} = 230, 250, \text{ and } 270$  MeV [16] has been used in a R(Q)RPA calculation of ISGMR in  $^{40}\text{Ca}$ ,  $^{56}\text{Fe}$ ,  $^{58}\text{Ni}$ ,  $^{60}\text{Ni}$ , and  $^{90}\text{Zr}$ . The resulting mean energies  $\bar{E}_3$  are plotted in the lower panel of Fig. 2, in comparison with data from Refs. [2,33,34]. We notice that while DD-ME2 and the  $K_{\text{nm}} = 250$  MeV effective interaction reproduce the experimental value  $\bar{E}_3$  for  $^{90}\text{Zr}$ , data in lighter nuclei are better described by the effective interaction with  $K_{\text{nm}} = 230$  MeV, except possibly for  $^{58}\text{Ni}$ , but for this nucleus the experimental energy  $\bar{E}_3$  differs considerably from the values in the neighboring  $^{56}\text{Fe}$  and  $^{60}\text{Ni}$  [2].

For the DD-ME2 effective interaction, the RHB+RQRPA isoscalar dipole transition strength distributions in  $^{56}\text{Fe}$ ,  $^{58}\text{Ni}$ , and  $^{60}\text{Ni}$  are shown in Fig. 3. In all three nuclei the E1 strength is strongly fragmented and distributed over a wide range of excitation energy between 10 MeV and 40 MeV, in agreement with the experimental results of Ref. [2]. Similarly to the results obtained for heavier nuclei [23,24,27], the E1 strength is basically concentrated in two broad structures: one in the region  $10 \text{ MeV} \leq E_x \leq 20 \text{ MeV}$ , and the high-energy component above 25 MeV and extending above 40 MeV excitation energy. Only the high-energy portion of the calculated E1 strength is sensitive to the nuclear matter compression modulus of the effective interaction. In a number

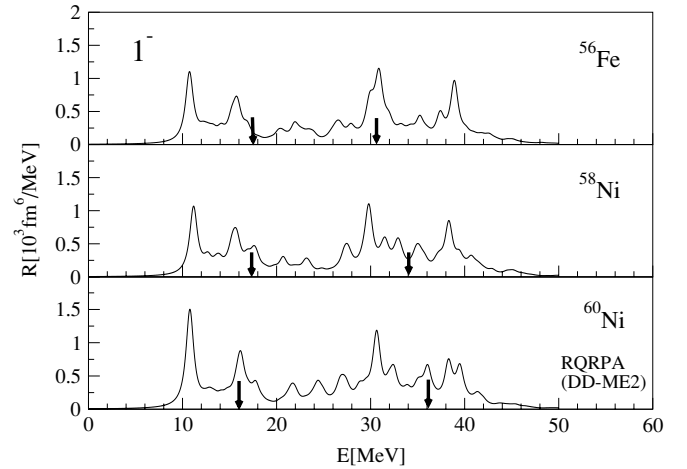


FIG. 3. The RQRPA(DD-ME2) isoscalar dipole transition strength in  $^{56}\text{Fe}$  and  $^{58,60}\text{Ni}$ . The experimental centroid energies of the low- and high-energy components are denoted by arrows [2].

of recent theoretical studies [25–27] it has been shown that the low-lying E1 strength mostly corresponds to vortical flow (dipole toroidal mode), although a strong mixture of compressional and vortical velocity fields is predicted in the intermediate and high-energy region.

In Fig. 3 the thick arrows denote the locations of the experimental centroid energies ( $m_1/m_0$ ) in the low- and high-energy regions of the isoscalar E1 strength in  $^{56}\text{Fe}$ ,  $^{58}\text{Ni}$ , and  $^{60}\text{Ni}$  [2]. These are compared in Fig. 4 with the theoretical values of the centroids of the low- and high-energy components, for different values of  $E_c$ , the somewhat arbitrary parameter which separates the low- and high-energy regions. We notice a good qualitative agreement between the calculated and experimental centroids in the high-energy region, especially taking into account that the E1 strength above  $E_x = 40$  MeV has not been observed in the experiment. In the low-energy region, however, the theoretical centroid energies are systematically

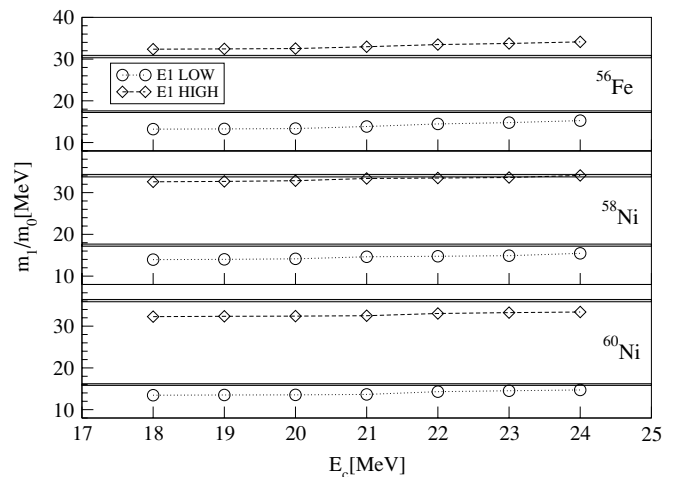


FIG. 4. Comparison of the RQRPA (circles and diamonds) and experimental (broad lines) [2] centroid energies of the low- and high-energy components of the E1 transition strength in  $^{56}\text{Fe}$  and  $^{58,60}\text{Ni}$  for different values of  $E_c$  (see text).

below the experimental values by  $\approx 1-4$  MeV, depending on the choice of  $E_c$ . This effect is in agreement with previous RRPAs calculations in heavier nuclei [27], and supports the picture of pronounced mixing between compressional and vorticity vibrations in the intermediate region of excitation energies.

In conclusion, we have performed RHB+RQRPA calculations of the isoscalar monopole and dipole strength distributions in  $^{56}\text{Fe}$ ,  $^{58}\text{Ni}$ ,  $^{60}\text{Ni}$  and compared the results with very recent experimental data [2]. For the ISGMR we find very good qualitative agreement between theory and experiment, both for the asymmetric shapes of the strength distributions, as well as for centroid ( $\bar{E}_1$ ) and mean energies ( $\bar{E}_3$ ). It has been noted, however, that while there is an excellent agreement between the ISGMR excitation energies calculated with DD-ME2 and the data for nuclei with  $A \geq 90$ , the theoretical centroids are systematically above the experimental values in lighter nuclei with  $A \leq 60$ . Even though because of asymmetric shapes and

pronounced fragmentation, ISGMR data in light nuclei are probably not very useful for extracting information on the nuclear matter compression modulus, we have shown that the ISGMR centroids in nuclei with  $A \leq 60$  are better described with an effective interaction similar to DD-ME2, but with a lower value of  $K_{\text{nm}} \approx 230$  MeV. The isoscalar E1 strength distributions calculated with DD-ME2 are in good agreement with the experimental results [2], and reproduce the observed bimodal structure with two broad components in the  $2\hbar\omega$  and  $3\hbar\omega$  energy regions. The calculated centroid energies of the low- and high-energy E1 components in  $^{56}\text{Fe}$ ,  $^{58}\text{Ni}$ , and  $^{60}\text{Ni}$  qualitatively reproduce the experimental values obtained from small-angle inelastic  $\alpha$ -scattering data.

This work has been supported in part by the Bundesministerium für Bildung und Forschung under project 06 TM 193, by the Gesellschaft für Schwerionenforschung (GSI) Darmstadt, and by the Alexander von Humboldt Stiftung.

- 
- [1] J. P. Blaizot, Phys. Rep. **64**, 171 (1980).  
 [2] Y.-W. Lui, D. H. Youngblood, H. L. Clark, Y. Tokimoto, and B. John, Phys. Rev. C **73**, 014314 (2006).  
 [3] R. C. Nayak *et al.*, Nucl. Phys. **A516**, 62 (1990).  
 [4] T. v. Chossy and W. Stocker, Phys. Rev. C **56**, 2518 (1997).  
 [5] V. M. Kolomietz and S. Shlomo, Phys. Rev. C **61**, 064302 (2000).  
 [6] I. Hamamoto, H. Sagawa, and X. Z. Zhang, Phys. Rev. C **56**, 3121 (1997).  
 [7] S. Shlomo and A. I. Sanzhur, Phys. Rev. C **65**, 044310 (2002).  
 [8] B. K. Agrawal, S. Shlomo, and V. Kim Au, Phys. Rev. C **68**, 031304(R) (2003).  
 [9] G. Colò, N. V. Giai, J. Meyer, K. Bennaceur, and P. Bonche, Phys. Rev. C **70**, 024307 (2004).  
 [10] J. Kvasil, N. Lo Iudice, Ch. Stoyanov, and P. Alexa, J. Phys. G **29**, 753 (2003).  
 [11] D. Lacroix, S. Ayik, and P. Chomaz, Phys. Rev. C **63**, 064305 (2001).  
 [12] S. Yildirim, T. Gaitanos, M. Di Toro, and V. Greco, Phys. Rev. C **72**, 064317 (2005).  
 [13] Z. Y. Ma *et al.*, Nucl. Phys. **A686**, 173 (2001).  
 [14] J. Piekarewicz, Phys. Rev. C **64**, 024307 (2001).  
 [15] J. Piekarewicz, Phys. Rev. C **66**, 034305 (2002).  
 [16] D. Vretenar, T. Nikšić, and P. Ring, Phys. Rev. C **68**, 024310 (2003).  
 [17] B. K. Agrawal, S. Shlomo, and A. I. Sanzhur, Phys. Rev. C **67**, 034314 (2003).  
 [18] B. K. Agrawal and S. Shlomo, Phys. Rev. C **70**, 014308 (2004).  
 [19] Tapas Sil, S. Shlomo, B. K. Agrawal, and P.-G. Reinhard, Phys. Rev. C **73**, 034316 (2006).  
 [20] G. Colò and N. Van Giai, Nucl. Phys. **A731**, 15 (2004).  
 [21] H. L. Clark, Y.-W. Lui, and D. H. Youngblood, Phys. Rev. C **63**, 031301(R) (2001).  
 [22] D. H. Youngblood *et al.*, Phys. Rev. C **69**, 054312 (2004).  
 [23] G. Colò, N. Van Giai, P. F. Bortignon, and M. R. Quaglia, Phys. Lett. **B485**, 362 (2000).  
 [24] D. Vretenar, A. Wandelt, and P. Ring, Phys. Lett. **B487**, 334 (2000).  
 [25] S. I. Bastrukov, S. Misicu, and V. I. Sushkov, Nucl. Phys. **A562**, 191 (1993).  
 [26] S. Misicu, Phys. Rev. C **73**, 024301 (2006).  
 [27] D. Vretenar, N. Paar, P. Ring, and T. Nikšić, Phys. Rev. C **65**, 021301(R) (2002).  
 [28] M. Uchida *et al.*, Phys. Lett. **B557**, 12 (2003).  
 [29] M. Uchida *et al.*, Phys. Rev. C **69**, 051301(R) (2004).  
 [30] N. Paar, P. Ring, T. Nikšić, and D. Vretenar, Phys. Rev. C **67**, 034312 (2003).  
 [31] D. Vretenar, A. V. Afanasjev, G. A. Lalazissis, P. Ring, Phys. Rep. **409**, 101 (2005).  
 [32] G. A. Lalazissis, T. Nikšić, D. Vretenar, and P. Ring, Phys. Rev. C **71**, 024312 (2005).  
 [33] D. H. Youngblood, Y. W. Lui, and H. L. Clark, Phys. Rev. C **55**, 2811 (1997).  
 [34] D. H. Youngblood, H. L. Clark, and Y.-W. Lui, Phys. Rev. Lett. **82**, 691 (1999).  
 [35] D. H. Youngblood *et al.*, Phys. Rev. C **69**, 034315 (2004).